

Magnetic behavior of single-crystal $\text{Co}(\text{SCN})_2(\text{CH}_3\text{OH})_2$: Three-dimensional Ising metamagnetism and field-induced spin reorientations

G. C. DeFotis, B. T. Wimberly, R. B. Jeffers, W. M. May, and T. M. Owens

Chemistry Department, College of William and Mary, Williamsburg, Virginia 23187-8795, USA

(Received 19 December 2006; revised manuscript received 11 May 2007; published 13 July 2007)

The magnetic behavior of single-crystal $\text{Co}(\text{SCN})_2(\text{CH}_3\text{OH})_2$ has been studied by dc susceptibility and magnetization measurements. Pronounced anisotropy in the susceptibility is present at all temperatures. Antiferromagnetic maxima appear in three orthogonal crystal susceptibilities at 4.45 ± 0.02 K. One of the axes, the monoclinic a^* direction of much the largest susceptibility, has the appearance of an easy axis and exhibits a transition at 4.15 ± 0.02 K. There are no indications of lower-dimensional behavior, probably because the spacing between SCN^- -coordinated layers of cobalt ions characterizing the structure is not large. A fit to the a^* susceptibility data using a high-temperature series expansion (HTSE) for the simple cubic three-dimensional Ising model yields $g=5.83$ and $J/k=0.49_0$ K; the positive sign indicates a dominant ferromagnetic interaction and large maximum susceptibility value, despite overall antiferromagnetism. A low-temperature series expansion fit for the same model, at temperatures below that of the susceptibility maximum, yields $g=5.79$ and $J/k=-0.63_5$ K. Along the same a^* axis magnetization versus field isotherms reveal an abrupt transition at 3.73 kG for 1.84 K, the magnetization then gradually approaching near saturation as a 15.9-kG field limit is approached. Along the two orthogonal b and c crystal axes much less abrupt transitions are observed in the several kG range, one transition along b and two along c . None have the appearance of transitions to a polarized paramagnetic state; they are believed to be spin reorientation in nature. Alternative scenarios for the transition along a^* are considered, spin-flop and metamagnetic. A mean-field analysis based on the former yields an exchange field $H_E=19.6$ kG and an anisotropy field $H_A=0.35$ kG. But this interpretation entails inconsistencies regarding the appearance of M vs H and conflicting estimates of the exchange interaction. Analysis based on the metamagnetic hypothesis yields for the interlayer antiferromagnetic exchange $J_2/k=-0.36_5$ K. In conjunction with the HTSE result, an intralayer ferromagnetic exchange $J_1/k=1.10$ K is inferred. The ordering temperature and Weiss parameter predicted from these exchange parameters, again on a mean-field basis, are reasonably consistent with observation. In either interpretation a multisublattice model with hidden canting suggests itself in order to rationalize the spin reorientation transitions along the b and c axes.

DOI: [10.1103/PhysRevB.76.014419](https://doi.org/10.1103/PhysRevB.76.014419)

PACS number(s): 75.30.Cr, 75.50.Ee, 75.30.Kz, 75.30.Et

I. INTRODUCTION

The systematic variation of a structural feature in a magnetic series where other elements are held constant—e.g., the identity of the magnetic ion—or contrastingly, varying a basic magnetic feature like the identity of the spin carrying metal ion while maintaining structural factors as similar as possible, can be a fruitful way of exploring magnetic behavior. A family of compounds which we have been studying for some time, and which lends itself to such variations, is $M(\text{SCN})_2(\text{ROH})_2$, where M is a divalent transition-metal ion (Mn^{2+} , Fe^{2+} , Co^{2+} , Ni^{2+}) and where different alcohols determined by the R group (CH_3 , C_2H_5 , $i\text{-C}_3\text{H}_7$, $n\text{-C}_3\text{H}_7$) can occur.¹⁻⁵ The materials are characterized by thiocyanate-coordinated layers of metal ions, with alcohols essentially between the layers and serving to separate them.⁶ Different metal ions exhibit different spin values and, usually even more important, are characterized by different degrees of spin anisotropy or even exchange anisotropy. The size of the alcohol will strongly influence interlayer separations. Thus, both Heisenberg and Ising systems of low lattice dimensionality have been identified in this family of compounds. Because the polynuclear thiocyanate ion is not a very common superexchange ligand, while interactions through such multiple-atom exchange mediators must be more complex

than through single-atom bridges, there is an additional element of interest in members of the present family.

We report here single-crystal susceptibility and magnetization measurements on $\text{Co}(\text{SCN})_2(\text{CH}_3\text{OH})_2$. Very pronounced anisotropic properties are observed, including some unusual features. Comparison can also be made with results obtained previously on single crystals of other compounds in the family. These include $\text{Co}(\text{SCN})_2(n\text{-C}_3\text{H}_7\text{OH})_2$, for which the interlayer separation is much larger, and $\text{Mn}(\text{SCN})_2(\text{CH}_3\text{OH})_2$, where the metal ion is much more isotropic.^{1,4}

II. EXPERIMENT

Anhydrous $\text{Co}(\text{SCN})_2$ was prepared as described previously,⁷ then dissolved in spectroscopic grade methanol and slowly evaporated in a desiccator over 3-Å molecular sieves. Crystals of $\text{Co}(\text{SCN})_2(\text{CH}_3\text{OH})_2$ were obtained, pale pink in color and typically in the form of relatively flat diamond-shaped prisms. Chemical analysis confirmed their chemical composition. The crystals cleaved easily parallel to the large flat face, similar to the behavior described for $\text{Mn}(\text{SCN})_2(\text{CH}_3\text{OH})_2$,⁴ suggesting a structure based on layers weakly coupled together chemically. Comparison with

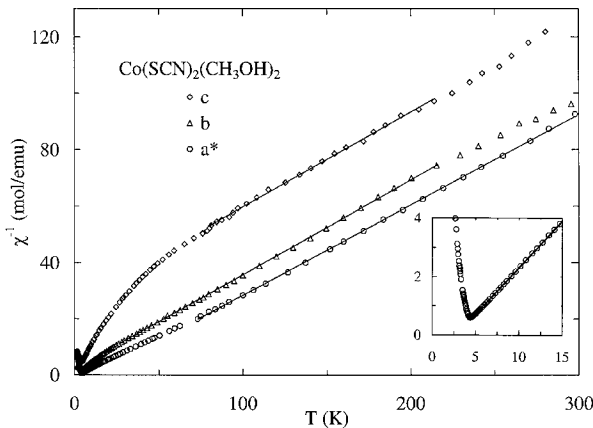


FIG. 1. Inverse molar susceptibility vs temperature for $\text{Co}(\text{SCN})_2(\text{CH}_3\text{OH})_2$ along three orthogonal crystal axes. Lines are Curie-Weiss fits described in the text. The inset shows the low- T linear regime, and Curie-Weiss fit, for the a^* axis.

predictions from the crystal structure⁸ for interfacial angles implied that, as for the methanol system, the crystal faces were those of the $\{011\}$ and $\{100\}$ forms, with the b - c plane the large flat face. By this method, the monoclinic b axis was identified as a short diagonal in the diamond face. The single crystal used in the magnetic measurements weighed 25.72 mg. To protect it during measurements, from either water absorption or loss of alcohol, it was coated with a thin layer of apiezon grease.

Magnetization and susceptibility measurements were made using a variable-temperature vibrating-sample-magnetometer system. Temperatures, measured with a carbon-glass resistance thermometer in close proximity to the sample, are estimated to be accurate to ± 0.010 – 0.20 K, depending on the range, with a precision substantially better than this. Magnetization and susceptibility data are estimated to be accurate to within 1.5%, also with yet better precision. Magnetic-field values are accurate to $\max(2 \text{ G}, 0.1\%)$. Susceptibilities displayed in the following have been corrected for diamagnetism and demagnetization. The former is estimated to be -126×10^{-6} emu/mol. The latter is a small correction because susceptibilities in this material are not very large.

III. MEASUREMENTS AND ANALYSIS

A. Magnetic susceptibility

In Fig. 1 appear the reciprocal molar susceptibilities of $\text{Co}(\text{SCN})_2(\text{CH}_3\text{OH})_2$ measured along three orthogonal axes of the monoclinic structure previously determined and described.⁸ The anisotropy is substantial throughout the temperature range, as is typical of $\text{Co}(\text{II})$ compounds. Although differing in detail, the inverse susceptibility versus T plot exhibits some similarity with that determined previously¹ for $\text{Co}(\text{SCN})_2(n\text{-C}_3\text{H}_7\text{OH})_2$ in that two of the inverse susceptibility sets differ from each other less than they do from a set along a third axis which shows the smallest susceptibility. Also, in each substance the largest susceptibility, hence

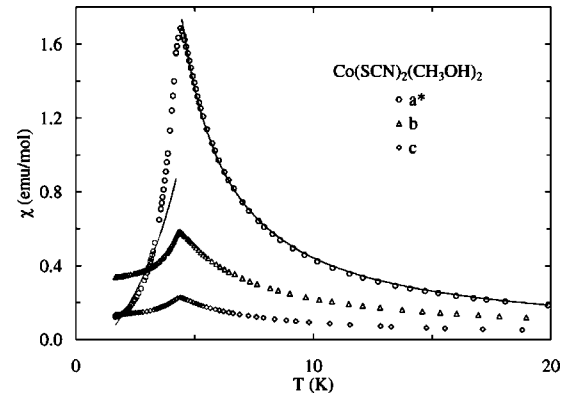


FIG. 2. Magnetic susceptibility vs temperature for $\text{Co}(\text{SCN})_2(\text{CH}_3\text{OH})_2$ along three orthogonal crystal axes. Curves through a^* data are HTSE and LTSE fits described in the text.

smallest inverse susceptibility, is that measured normal to the crystal cleavage plane.

Curvature in the reciprocal susceptibility versus T plot is evident for each of the axes, at temperatures below about 25 K for b and, remarkably, below about 70 K for a^* and 80 K for c . At high temperatures deviations from linearity appear for the b and c axes especially, probably from a combination of small signal size and imperfect thermal equilibrium at the highest T . Each of the lower-temperature limits for the main quasilinear behavior is far higher than the antiferromagnetic transition signaled by the data presented next. However, at high temperatures contributions to the susceptibility arise from excited doublets among the six resulting, via crystal field distortions and spin-orbit coupling, from the ${}^4T_{1g}$ Co^{2+} octahedral ground term. In the previously examined $\text{Co}(\text{SCN})_2(n\text{-C}_3\text{H}_7\text{OH})_2$ it was only along the axis normal to the cleavage plane that a linear $\chi^{-1}(T)$ dependence appeared. Fits to data in each of the indicated linear regimes lead to Curie and Weiss constants in $\chi = C/(T - \theta)$ of 3.13 emu K/mol and 11.0 K for a^* , 2.98 emu K/mol and -6.6 K for b , and 2.97 emu K/mol and -77.5 K for c ; these are represented by the corresponding lines through the data in Fig. 1. It is significant to note that excellent linearity also obtains for the a^* data in the low-temperature range 6–15 K. A fit here yields $C = 3.11$ emu K/mol, very similar to the high-temperature result, and a much smaller but still positive $\theta = 2.82$ K.

In Fig. 2 appear the susceptibilities along the same three orthogonal axes for relatively low temperatures. Very pronounced anisotropy is evident. The b and c axes were found by experiment to be of maximum and minimum susceptibilities, respectively, in the cleavage plane of the crystal. The a^* susceptibility, measured normal to the b - c cleavage plane, is much the largest and tends to a value close to zero as T approaches zero, suggesting that a^* is an antiferromagnetic easy axis. While there is uncertainty as to the size of $\chi_{a^*}(0)$, it is unlikely that the value is larger than a few 0.01 emu/mol. Notable is that neither the b - nor c -axis susceptibility has the standard appearance (near constancy for temperatures below that of the susceptibility maximum) of a perpendicular susceptibility in an ordered antiferromagnet.

The maximum in χ_{a^*} occurs at 4.45 ± 0.02 K, and a maximum in the derivative $d\chi/dT$ can be identified at 4.15 ± 0.02 K. The latter feature is the theoretical location of the ordering temperature. Within the precision of the measurements the maxima in the b - and c -axis susceptibilities occur at the same temperature as for the a^* axis, but there is no indication of any $(d\chi/dT)_{\max}$ in χ_b or χ_c .

It is possible that the easy axis and perpendiculars to it have not been located exactly. This is difficult to do if these axes are not conveniently located in the b - c crystal cleavage plane and normal to it. If one assumes that χ_{a^*} is tending not to 0 as $T \rightarrow 0$ but to a value like 0.03 emu/mol (the largest we think plausible from the data), then analysis of the observed susceptibilities via a standard $\chi(\varphi) = \chi_{\parallel} \cos^2 \varphi + \chi_{\perp} \sin^2 \varphi$ form, and assuming that the perpendicular susceptibilities are actually constant below T_N , suggests that the easy axis could be 10° – 15° from a^* . Even in such a case the anisotropy between the parallel and perpendicular susceptibilities would be comparable with that exhibited in Fig. 2. An alternative to the misorientation hypothesis is that the ordered magnetic arrangement does not have a single easy axis of spin alignment.

The very large size of one crystal axis susceptibility compared to the other two suggests Ising model behavior, which is common in Co(II) systems. Although two-dimensional magnetic behavior readily arises in the $M(\text{SCN})_2(\text{ROH})_2$ family, as in $\text{Co}(\text{SCN})_2(n\text{-C}_3\text{H}_7\text{OH})_2$, it is least likely to do so when the smallest alcohol, CH_3OH , is involved, leading to the smallest separations between metal-thiocyanate layers. Rather good evidence for the absence of two-dimensional behavior in the present system is the ratio $T_c/T(\chi_{\max}) = 0.93$. This is in the range typical of three-dimensional magnets and decidedly too high for a quasi-two-dimensional system. Also, the maximum in the a^* susceptibility does not look particularly broad, arguing against lower dimensionality.

The a^* susceptibility, above and below the temperature of the maximum, was fit with high- and low-temperature series expansions, respectively, for the three-dimensional Ising model on a simple cubic lattice with $S = \frac{1}{2}$.^{9,10} These are the curves shown in Fig. 2. The high-temperature series expansion (HTSE) fit, from 4.5 to 50 K, has an rms deviation of 2.2% and seems acceptable; the fit parameters are $g = 5.83_0$ and $J/k = 0.49_0$ K. The low-temperature series expansion (LTSE) fit, from 1.5 to 3.75 K, has an rms deviation of 16.2%, with fit parameters $g = 5.78_7$ and $J/k = -0.63_5$ K. It is evidently distinctly poorer. The numbers cited are with the exchange interaction convention $\hat{H}_{\text{ex}} = -2J \sum_{i>j} \hat{S}_i \cdot \hat{S}_j$. The large g values are typical of the Ising axis with an effective $S' = \frac{1}{2}$.

That the HTSE fit yields a positive J despite the obvious antiferromagnetic nature of the behavior is a result of a strongly increasing susceptibility as the unusually large value of χ_{\max} is approached on decreasing the temperature. Evidently the strongest interactions in $\text{Co}(\text{SCN})_2(\text{CH}_3\text{OH})_2$ are ferromagnetic. Naturally, an increasing susceptibility with increasing temperature, as fit by the LTSE, is consistent only with antiferromagnetism and, hence, a negative J in this case. It is tempting to conclude already at this stage (although, as will emerge later, this is unexpected) that there

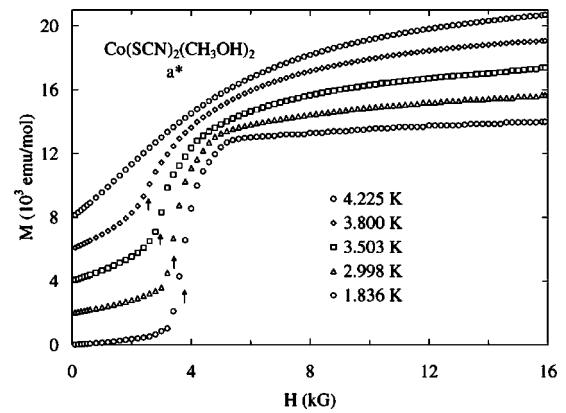


FIG. 3. Molar magnetization vs field for $\text{Co}(\text{SCN})_2(\text{CH}_3\text{OH})_2$ along a^* at various temperatures. Arrows indicate estimated locations of field-induced transitions. For clarity successively higher-temperature data are shifted up 2, 4, 6, and 8×10^3 emu/mol.

occur in this system ferromagnetically coupled layers which interact with each other antiferromagnetically.

B. Magnetization

In Figs. 3–5 appear magnetization versus field isotherms along the three orthogonal crystal directions already indicated in Figs. 1 and 2. The a^* direction, and presumptive easy axis, displays the most pronounced field-induced transition and one sharp enough that first-order behavior is suggested. Transition features are more gradual along the b and c axes, and also characterized by lesser increases in the magnetization value than along a^* (and with transitions along c weaker than along b). Notably, there appear successive transitions separated by a few kG along c . While 4.2-K isotherms are shown, clear anomalies corresponding to transitions cannot be identified. This temperature is slightly above the ordering temperature inferred from susceptibility data.

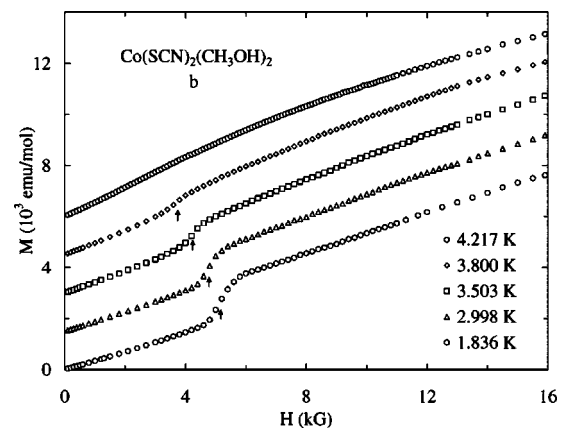


FIG. 4. Molar magnetization vs field for $\text{Co}(\text{SCN})_2(\text{CH}_3\text{OH})_2$ along b at various temperatures. Arrows indicate estimated locations of field-induced transitions. For clarity successively higher-temperature data are shifted up 1.5, 3.0, 4.5, and 6.0×10^3 emu/mol.

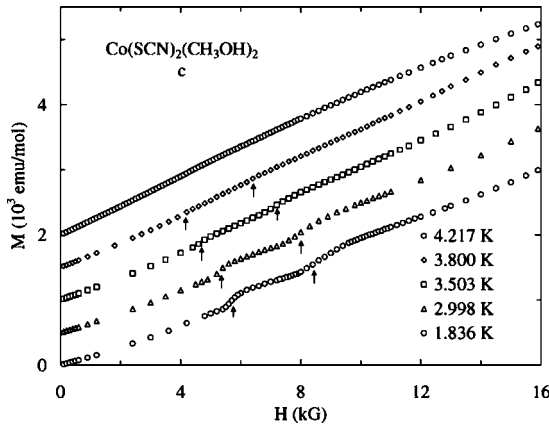


FIG. 5. Molar magnetization vs field for $\text{Co}(\text{SCN})_2(\text{CH}_3\text{OH})_2$ along c at various temperatures. Arrows indicated estimated locations of field-induced transitions. For clarity successively higher-temperature data are shifted up 0.5, 1.0, 1.5, and 2.0 $\times 10^3$ emu/mol.

In Fig. 6 are shown the transition fields versus temperature for the three axes. A smooth variation of increasing field with decreasing temperature is apparent for each separately identified transition. Along the easy axis of a weak to moderately anisotropic antiferromagnet a first-order spin-flop transition is expected, followed at higher field by a second-order transition to a highly polarized paramagnetic phase. These transitions should appear as near vertical jumps in M vs H and levelings of M vs H , respectively. It seems likely that the latter condition has not yet been attained in the isotherms of Fig. 3, though the slope of $M(H)$ has decreased substantially near 16 kG. An objection to a spin-flop interpretation is that the expected sudden change (following the jump in M) to a lesser M vs H slope but one still much larger than zero, persisting over a substantial field range until leveling sets in, is not seen. Nevertheless, in order to illustrate the difficulties which arise, an analysis based on the spin-flop scenario will be presented.

The behaviors along b and c differ in location of the most obvious transition along each axis and, more especially, in

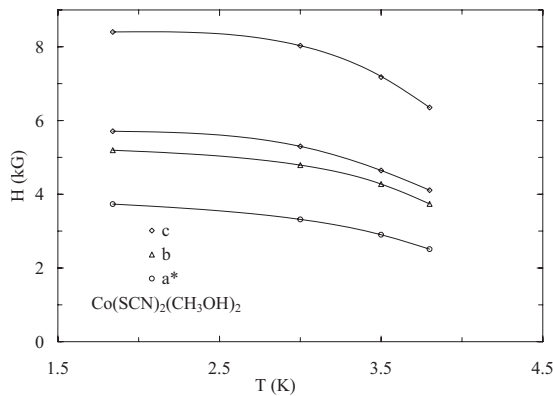


FIG. 6. Observed transition fields along three orthogonal crystal axes in $\text{Co}(\text{SCN})_2(\text{CH}_3\text{OH})_2$ vs temperature. Curves through results are guides to the eye only.

the occurrence of successive transitions along c . For a direction perpendicular to the easy axis one normally expects a single transition and at a larger field than any spin-flop transition along the easy axis. The transition field along the b axis is somewhat larger at each temperature than that along the a^* axis. Along the c axis the transition fields are somewhat larger yet. However, as will be seen below, the observed transitions along b or c cannot be identified with a standard hard-axis critical field; nor do they have the expected appearance of such.

Mean-field theory applied to a weakly anisotropic two-sublattice antiferromagnet yields expressions, strictly valid at 0 K, for the spin-flop field H_{SF} , the critical field H_c for the second-order transition to the paramagnetic state, and the corresponding critical field H'_c when the applied field is perpendicular to the easy axis¹¹:

$$H_{\text{SF}} = (2H_E H_A - H_A^2)^{1/2}, \quad (1)$$

$$H_c = 2H_E - H_A, \quad (2)$$

$$H'_c = 2H_E + H_A, \quad (3)$$

in terms of the effective exchange and anisotropy fields H_E and H_A . With the exchange interaction convention noted earlier, the exchange and anisotropy fields can be expressed in terms of microscopic parameters as $H_E = 2z|J|S/g\mu_B$ and $H_A = 2|D|S/g\mu_B$, where z is the number of interacting neighbors and D is a local anisotropy constant, typically in a single-ion form like $D\hat{S}_z^2$.

In principle it should be possible to distinguish between the two perpendicular directions, which may be characterized by different anisotropy constants, yet this is very rarely done. Distinctly different behavior occurs along the b and c axes of $\text{Co}(\text{SCN})_2(\text{CH}_3\text{OH})_2$, which if not quite true perpendicular directions are not very far removed. Since we do not clearly observe the H_c transition along the a^* axis, Eqs. (1) and (2) cannot be employed simultaneously to solve for H_E and H_A . The possibility of using Eqs. (1) and (3) instead suggests itself. But a problem is encountered if one takes any of the transition fields along b or c as an H'_c in Eq. (3) in conjunction with the assumed spin-flop transition fields observed along a^* . The former are too small to yield acceptable (i.e., physical, real) solutions for the effective fields. This is not surprising since any H'_c value should be larger than any H_c value according to Eqs. (2) and (3). The field-induced transitions along b and c represent something other than second-order transitions to the paramagnetic state. Nor can their appearance, location, and number (2 along c) be explained by modest misorientations of the axes—i.e., a^* not quite the easy axis, b and c not quite two perpendicular axes.

Another expression from mean-field theory can be employed in order to estimate the effective fields. With the effect of anisotropy included the 0 K value of the perpendicular susceptibility is expressible as¹¹

$$\chi_{\perp}(0) = 2M_S/(2H_E + H_A), \quad (4)$$

where M_S is the saturation magnetization of an antiferromagnetic sublattice, $M_S = N_0 g \mu_B S/2$ with N_0 Avogadro's number.

The value of $\chi_{\perp}(0)$ will be taken to be the average of the peak values of susceptibility along the b and c axes, 0.41 emu/mol. With an effective spin of $\frac{1}{2}$ in the helium temperature range, the g value will be taken as the average of those from the HTSE and LTSE fits shown in Fig. 2, 5.81 (virtually the same as the $g=5.78$ emerging from Curie-Weiss fitting of χ_{a^*} at higher temperatures using the standard expression for the Curie constant $C=N_0g^2\mu_B^2S(S+1)/3k$, with $S=\frac{1}{2}$ and fitted $C=3.13$ emu K/mol). Substituting in Eq. (4) yields $2H_E+H_A=39.6$ kG.

The above result can be combined with Eq. (1), taking the estimated spin-flop field at 1.84 K as sufficiently close to that at 0 K. Employing the observed $H_{SF}=3.73$ kG yields a quadratic equation in H_A with two solutions, 19.4 kG and 0.35 kG. The former looks much too large for an anisotropy field, would yield via the result at the end of the previous paragraph a smaller exchange field of 10.1 kG, and (most unacceptable) would yield via Eq. (2) an impossibly small H_c of 0.8 kG. The alternative $H_A=0.35$ kG is plausible for a Co(II) system and yields an also plausible $H_E=19.6$ kG. The consequent H_c is much larger than 16 kG, which may be consistent with Fig. 3 though the shape of M vs H is not as expected in the spin-flop scenario.

The alternative interpretation and analysis of the field induced transition along a^* is that of metamagnetism. Such a transition is first order in nature, as the a^* magnetization data suggest. The standard scenario for metamagnetism involves an intrasublattice ferromagnetic exchange and anisotropy that is stronger than the intersublattice antiferromagnetic exchange. For sufficient applied field, the latter exchange tendency is overcome and sublattices become ferromagnetically aligned; the anisotropy is equally satisfied by spin alignment along a given direction or its opposite. In $\text{Co}(\text{SCN})_2(\text{CH}_3\text{OH})_2$ the possibility of ferromagnetic interactions within the Co-SCN layers and antiferromagnetic between the layers is a natural scenario for metamagnetism. Strong anisotropy is typical of Co(II) ions. Mean-field theory applied to an antiferromagnet of such type yields an expression for the metamagnetic critical field: $H_c=AM$, where M is the sublattice magnetization $N_0g\mu_B S/2$ and A is a mean-field coefficient given by $4z_2|J_2|/N_0g^2\mu_B^2$, with z_2 and J_2 the number of neighbors involved and the interlayer antiferromagnetic interaction, respectively.¹² The exchange interaction convention is as before and substitution yields

$$H_c = 2z_2|J_2|S/g\mu_B. \quad (5)$$

Employing the average g value from the a^* susceptibility fits, $g=5.81$, effective spin $S=\frac{1}{2}$, and the 1.84 K critical field along a^* of 3.73 kG, there results $z_2|J_2|=1.46$ K (it is understood that antiferromagnetic J_2 is negative.) Based on the structure of $\text{Co}(\text{SCN})_2(\text{CH}_3\text{OH})_2$, it is likely that there are $z_2=4$ effective interplanar neighbors of near equivalency. Hence $J_2/k=-0.365$ K. This value is somewhat less negative than the interaction emerging from the not very satisfactory LTSE fit.

IV. DISCUSSION

The comparative magnetic behavior implies that $\text{Co}(\text{SCN})_2(\text{CH}_3\text{OH})_2$ is definitely more three dimensional

than the previously studied $\text{Mn}(\text{SCN})_2(\text{CH}_3\text{OH})_2$. While various perspective views of the two crystal structures^{4,8} appear very similar, there are small but significant differences in detail. The most important of these is undoubtedly that between adjacent b - c -plane metal-thiocyanate-coordinated layers, the closest metal-metal distances are 7.252 Å between cobalt ions but 7.817 Å between manganese ions. This is a huge difference compared to the very modestly greater interlayer (normal) separation of 7.233 Å in the cobalt system versus 7.222 Å in the manganese. A similarly modest difference in interlayer sulfur-sulfur contact distances (the sulfur atoms stick out of the planes referred to, defined by the cobalt ions, and thus come closer together) of 3.980 Å in the cobalt material versus 3.964 Å in the manganese must also be of less importance than the decidedly smaller interlayer cobalt separations. There is a more compact metal-thiocyanate connectivity in $\text{Co}(\text{SCN})_2(\text{CH}_3\text{OH})_2$. The overall size of the SCN^- ions in the cobalt and manganese systems is virtually identical, 2.800 Å and 2.806 Å, respectively, from S to N. But the M -S and M -N bond distances (each metal ion is coordinated to four SCN^- ions, two each via the alternate bonding modes involving the end atoms of the thiocyanate ion) are significantly shorter in the cobalt material (2.595 Å and 2.064 Å, respectively) than in the manganese (2.733 Å and 2.135 Å, respectively). Interlayer exchange most plausibly occurs via a Co-S \cdots S-C-N-Co pathway, as in the analogous manganese system, and is similarly likely to be antiferromagnetic because of fairly large bond angles along this pathway. It was estimated⁴ that in $\text{Mn}(\text{SCN})_2(\text{CH}_3\text{OH})_2$ the interlayer interaction is about 23% the size of the intralayer. The shorter atom-atom distances along the indicated pathway in $\text{Co}(\text{SCN})_2(\text{CH}_3\text{OH})_2$ can be expected to boost the interlayer exchange substantially, leading to virtual absence of lower dimensional magnetic behavior.

The exchange interaction from the simple cubic (sc) HTSE Ising model fit to the a^* susceptibility represents an average net interaction in the system, not simply a ferromagnetic intralayer exchange. Antiferromagnetic interactions necessarily occur as well, with the interlayer interaction deduced on the metamagnetic hypothesis presumably dominant. Since six neighbors are assumed in the sc HTSE fit, the total net interaction operating is $6(0.490 \text{ K})=2.94$ K. Based on the structural considerations already reviewed one can identify four essentially equivalent intralayer exchange pathways connecting cobalt ions and four quite different interlayer pathways. The antiferromagnetic interlayer interaction has been estimated as $J_2/k=-0.365$ K, with $z_2=4$ assumed. Hence the effective intralayer ferromagnetic interaction operating, with $z_1=4$, can be plausibly estimated as $[2.94 \text{ K} - 4(-0.365 \text{ K})]/4=1.10$ K.

The exchange interactions in $\text{Co}(\text{SCN})_2(\text{CH}_3\text{OH})_2$, inferred on the above basis, are of similar size (though somewhat larger in magnitude) to those determined previously for $\text{Mn}(\text{SCN})_2(\text{CH}_3\text{OH})_2$,⁴ where in this somewhat more two-dimensional material an intralayer exchange of -0.70 K and an interlayer exchange of -0.16 K emerged. The larger size exchange interactions in the cobalt material must be due, in significant measure, to the generally tighter packing in

the cobalt than the manganese system. But somewhat surprising is existence of a dominant interaction here which is ferromagnetic. Antiferromagnetic interactions are much more common in general and also tend to be favored when the d shell is half-filled or more. It is hard to understand, based on the modest differences in atom-atom separations and bond angles between $\text{Mn}(\text{SCN})_2(\text{CH}_3\text{OH})_2$ and $\text{Co}(\text{SCN})_2(\text{CH}_3\text{OH})_2$ and familiar magnetostructural correlations (like linear or near linear bridges favoring antiferromagnetic exchange), why a change in the sign of the main intralayer interaction occurs from the manganese to the cobalt system. However, the best established magnetostructural correlations are derived from studies of systems with simpler superexchange pathways than the multiatom bridges with several bond angles involved in the present compound.

The previously studied manganese analog displayed the expected Heisenberg model behavior. Certain relations among T_{\max} , χ_{\max} and J derived from HTSEs for the two-dimensional (2D) and three-dimensional $S=5/2$ Heisenberg models were testable, favoring a quasi-2D interpretation.⁴ Precisely analogous relations for the 3D-Ising model are not so apparent in the literature, but some theoretical results are available for comparison. Thus the observed ratio of $T_c/T_{\max}=4.15\text{ K}/4.45\text{ K}=0.93_3$ is quite similar to theoretical results for the 3D-Ising model, 0.911 and 939 on simple cubic and body-centered-cubic lattices, respectively.¹⁰ Two-dimensional Ising model results for this ratio are far lower.¹³ Employing the a^* data (most resembling an easy axis) the ratio of χ_{\max} to $\chi(T_c)$ is 1.20₄. The three-dimensional sc and bcc predictions are 1.028 and 1.017, respectively.¹⁰ The observed ratio is larger than but substantially closer to these values than to much larger ones for the 2D-Ising model.¹³

Certain results are also available which relate T_c to J for the 3D-Ising model. For an $S=1/2$ Ising model on cubic lattices, the following values of the ratio kT_c/zJ have been determined: 0.75180, 0.79416, and 0.81627 for the sc, bcc, and fcc (face-centered-cubic) lattices, with $z=6, 8,$ and 12 interacting neighbors, respectively.¹⁴ The convention here involves a J value half the size of that used in this paper. From these results and dividing by 2 the $J/k=0.49_0\text{ K}$ from the HTSE fit earlier the calculated T_c values are 1.10₅ K, 1.55₇ K, and 2.40 K, respectively. All are well below the observed 4.15 K. Had series been used for the more highly coordinated bcc and fcc lattices the resulting J value would almost certainly have been smaller in magnitude; hence, the second and third T_c values above are probably overestimates. It is common for T_c calculated from series-expansion-derived J values to be low, since the effects of anisotropy, which typically enhance T_c , are normally not included in such expansions. This has been considered in detail for certain $S=3/2$ Fe(III) systems.¹⁵ Although the formal Co(II) spin here is the same, the nature of the anisotropy is different, not arising from a zero-field splitting. There probably exists a genuine exchange anisotropy even at not so low temperatures, because of the splitting of the free ion term into six Kramers doublets. It is less evident how to assess the effect on T_c in such a case.

Another comparison is with results of series expansions for higher spin values, $S=3/2$ in particular. The ratio of kT_c/J'

has been obtained for the Ising model on a sc lattice for various spin values.¹⁶ In this expression J' is defined as $2S^2J$ where J is in this paper's convention. For $S=1/2$ the ratio is 4.5060 and this leads to the same sc case result for the $S=1/2$ model given in the previous paragraph. For $S=3/2$ the ratio is 2.7127. With $J/k=0.49_0\text{ K}$ the result is $T_c=5.98\text{ K}$. An objection is that the J/k value should be smaller on a spin- $3/2$ basis, several times so. Hence, it is very likely that T_c remains underestimated without of a detailed accounting of the effects of exchange anisotropy.

One can also employ standard mean-field theory results for the two-sublattice antiferromagnet,¹⁷

$$T_N = [2S(S+1)/3k][z_1J_1 - z_2J_2], \quad (6)$$

where J_1 and J_2 are intrasublattice and intersublattice interactions in the same exchange Hamiltonian convention employed in this paper. Substituting the previously inferred values $J_1/k=1.10\text{ K}$, $J_2/k=-0.36_5\text{ K}$ along with $z_1=4=z_2$, and the same effective $S=1/2$ assumed in deducing these J values, there results $T_N=2.93\text{ K}$. The contrasting-sign J_1 and J_2 values operate to enhance T_N relative to a case where both interactions are the same sign (negative), as is expected physically. The result, while still low, is closer to the observed ordering temperature than were the estimates in the previous paragraphs. In the same approximation the expression for the Weiss parameter is

$$\theta = [2S(S+1)3k][z_1J_1 + z_2J_2], \quad (7)$$

whereupon substitution of the same values yields $\theta=1.47\text{ K}$. As noted in Sec. III A, fitting the a^* data in the lowest-temperature range where plausible linearity exists yields $\theta=2.82\text{ K}$, along with $C=3.11\text{ emu K/mol}$, and so $g=5.76$ on an $S=1/2$ basis. Agreement with the θ value calculated from Eq. (7) is reasonable.

In the spin-flop scenario a transition to a fully polarized paramagnetic state should occur substantially higher than we can measure, near a value $H_c=2H_E-H_A=2(19.6\text{ kG})-0.35\text{ kG}=38.9\text{ kG}$, along the a^* direction. The full saturation moment expected can be estimated using the HTSE-fit g value (5.83) with $S=1/2$ as $g\mu_B S$ per ion or $2.92\mu_B/\text{ion}$. The slightly lower g values (5.76, 5.78, 5.79) from the Curie-Weiss fits or the LTSE fit to the a^* data lead to a very similar $2.89\mu_B/\text{ion}$. The largest magnetization observed along a^* , at 15.9 kG and 1.836 K, is $14.0 \times 10^3\text{ emu/mol}$, or $2.51\mu_B/\text{ion}$. This is 86% of the saturation value, fairly close to it. Both this fact and the appearance of $M(H)$ along a^* are more consistent with a metamagnetic interpretation of the a^* transition than the spin-flop scenario.

If one accepts the H_E value (spin-flop scenario) inferred in Sec. III B, 19.6 kG, and employs the mean-field expression noted earlier ($H_E=2z|J|S/g\mu_B$), along with $g=5.83$ and $z=6$ from the sc HTSE fit, there results $|J|/k=1.28\text{ K}$. This is over 2 times larger than the magnitude of J emerging from the same fit. Moreover, in the spin-flop context a negative, antiferromagnetic exchange must be assumed, in contrast to the ferromagnetic exchange in the HTSE fit. Nor does it make sense to compare favorably the 1.28-K exchange interaction with the deduced ferromagnetic intralayer exchange in

the metamagnetic scenario, since the bases for the two estimates are inconsistent. Calculating H_E from the fitted $J/k = 0.49_0$ K gives 7.50 kG and from the presumed spin-flop field an associated $H_A = 0.99$ kG. While the latter may be possible, the H_E value is too small, since Eqs. (2) and (3) then yield critical fields which could have been observed, but were not.

As noted previously, the three orthogonal single-crystal susceptibilities in Fig. 2 are not quite standard in appearance as a parallel and two perpendicular antiferromagnetic susceptibilities. Although modest misorientations are a possible explanation, the evidence of all the data suggests as more likely the absence of a single easy axis of spin alignment. The crystal structure facilitates this possibility, with two pairs of cobalt centers per unit cell that are not exactly equivalent (inversion centers exist which relate cobalt centers of each pair but not between the pairs). In $\text{Mn}(\text{SCN})_2(\text{CH}_3\text{OH})_2$ and $\text{Mn}(\text{SCN})_2(\text{C}_2\text{H}_5\text{OH})_2$ spin canting allowed by the same crystal symmetry, and believed to be a consequence of small single-ion anisotropy, was observed. Canting was also observed in $\text{Co}(\text{SCN})_2(n\text{-C}_3\text{H}_7\text{OH})_2$, for which the structure is not yet determined. In $\text{Co}(\text{SCN})_2(\text{CH}_3\text{OH})_2$ no evidence of canting and associated weak ferromagnetic moment is apparent. The possibility of hidden canting involving more than two sublattices arises, however.

Hidden canting also offers a potential explanation of the unusual pattern of field-induced transitions along the b and c axes. It is possible that the transitions along the b and c axes are field-induced spin reorientations. Natural molecular spin anisotropy axes are the linear or near linear O-Co-O, S-Co-S, and N-Co-N coordination bonds. These are not simply parallel or perpendicular to the measured crystal directions, and there are two slightly differently oriented sets of such axes per unit cell. The magnetic structure in the low-field antiferromagnetic state, as influenced by local anisotropies, could be complicated. This would create the possibility of inducing modest spin reorientations in small to moderate fields, with the nature and even number of such reorientations dependent on direction—e.g., one such along b but two along c .

The metamagnetic scenario led to an estimate for the interlayer antiferromagnetic exchange of $J_2/k = -0.36_5$ K. This result is taken in association with the evidence of ferromagnetic interactions from the HTSE a^* susceptibility fit, as well as the positive θ value along a^* . The appearance of $M(H)$ along a^* is also more suggestive of metamagnetism than in the spin-flop scenario, with a rise to a near saturation value over a moderate field range. And in the metamagnetic scenario the observed critical temperature and Weiss parameter are better accounted for.

In the metamagnetic scenario a spin structure with hidden canting and consequent field-induced transitions could still occur presumably, similarly rationalizing the features in $M(H)$ along the b and c axes. This appears much more plausible than attempting to account for these (although the second transition along c cannot be) by invoking modest misorientation and identification of a^* as the easy axis, together with the relation $H_c = H_{c0}/\cos \varphi$, where H_{c0} is the critical field along the true easy axis, H_c is that actually observed, and φ is the angle between the actual measurement direction and the true easy axis.¹² A discrepancy of 15° or less would push the critical field which should be observed along b or c to near or beyond the 15.9-kG magnet limit, contrary to observation. In order to yield the actual b - or c -axis critical fields via the above relation an unreasonably large misorientation of over 40° is needed; nor is the much reduced prominence of the transitions along these axes relative to a^* accounted for.

A neutron determination of the ordered magnetic structure would assist greatly in assessing the likelihood of the hidden canting hypothesis. It should be considered attractive since the behavior in the present system does not appear to have analogs in any other material we are familiar with.

ACKNOWLEDGMENT

Acknowledgment is made to the Donors of the American Chemical Society Petroleum Research Fund for the support of this research.

- ¹G. C. DeFotis, C. K. Barlowe, and W. R. Shangraw, *J. Magn. Magn. Mater.* **54-57**, 1493 (1986).
- ²G. C. DeFotis, E. M. McGhee, K. R. Echols, and R. S. Wiese, *J. Appl. Phys.* **63**, 3569 (1988).
- ³G. C. DeFotis, B. T. Wimberly, and E. M. McGhee, *J. Phys. (Paris), Colloq.* **49**, C8-855 (1988).
- ⁴G. C. DeFotis, E. D. Remy, and C. W. Scherrer, *Phys. Rev. B* **41**, 9074 (1990).
- ⁵G. C. DeFotis, E. W. Harlan, E. D. Remy, and K. D. Dell, *J. Appl. Phys.* **69**, 6004 (1991).
- ⁶J. N. McElearney, L. L. Balagot, J. A. Muir, and R. D. Spence, *Phys. Rev. B* **19**, 306 (1979).
- ⁷C. D. Flint and M. Goodgame, *J. Chem. Soc. A* **1970**, 442.
- ⁸G. C. DeFotis, E. M. Just, V. J. Pugh, G. A. Coffey, B. D. Hogg, S. L. Fitzhenry, J. L. Marmorino, D. J. Krovich, and R. V.

- Chamberlain, *J. Magn. Magn. Mater.* **202**, 27 (1999).
- ⁹M. F. Sykes, D. S. Gaunt, P. D. Roberts, and J. A. Wyles, *J. Phys. A* **5**, 640 (1972).
- ¹⁰M. E. Fisher and M. F. Sykes, *Physica (Utrecht)* **28**, 939 (1962).
- ¹¹L. J. deJongh and A. R. Miedema, *Adv. Phys.* **23**, 1 (1974).
- ¹²J. Kanamori, *Prog. Theor. Phys.* **20**, 890 (1958).
- ¹³M. F. Sykes and M. E. Fisher, *Physica (Utrecht)* **28**, 919 (1962).
- ¹⁴C. Domb, in *Phase Transitions and Critical Phenomena*, edited by C. Domb and M. S. Green (Academic, New York, 1974), Vol. 3.
- ¹⁵G. C. DeFotis, B. K. Failon, F. V. Wells, and H. H. Wickman, *Phys. Rev. B* **29**, 3795 (1984).
- ¹⁶W. J. Camp and J. P. Van Dyke, *Phys. Rev. B* **11**, 2579 (1975).
- ¹⁷F. Keffer, *Encyclopedia of Physics* (Springer-Verlag, New York, 1966), Vol. XVIII/2, Sec. B.